Water Research 283 (2025) 123683

Contents lists available at ScienceDirect

Water Research

journal homepage: www.elsevier.com/locate/watres

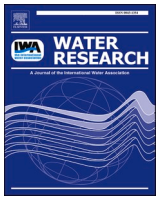

Uncovering microbial interactions in a persistent *Planktothrix* bloom: Towards early biomarker identification in hypereutrophic lakes

Mashuk Siddiquee [a], Sara Cornelius [a], Youngwoo Seo [a,b], George S. Bullerjahn [c], Thomas B. Bridgeman [d], Mike Sudman Jr. [e], Dae-Wook Kang [a,*]

[a] Department of Civil and Environmental Engineering, The University of Toledo, OH, 43606, USA
[b] Department of Chemical Engineering, The University of Toledo, OH, 43606, USA
[c] Department of Biological Sciences, Bowling Green State University, Bowling Green, OH 43403, USA
[d] Department of Environmental Sciences and Lake Erie Center, The University of Toledo, 6200 Bayshore Drive, OR, OH 43616, USA
[e] Celina Water Treatment Plant, 714 S Sugar St. Celina, OH 45822, USA

ARTICLE INFO

Keywords:
CyanoHABs
Planktothrix
Grand Lake St. Marys
Microbial dynamics
Metagenomics

ABSTRACT

Cyanobacterial harmful algal blooms pose significant threats to global water supplies, ecosystems, and economies. Among the harmful cyanobacteria, *Planktothrix,* a resilient and toxin-producing filamentous cyanobacterium, has garnered increasing attention. However, an understanding of the entire microbiome, particularly the phycosphere surrounding *Planktothrix* blooms, remains largely unexplored. To the best of our knowledge, this is the first comprehensive study combining 16S rDNA and fungal internal transcribed spacer amplicon sequencing and shotgun metagenomics to elucidate *Planktothrix* bloom microbiomes and identify potential microbial or functional biomarkers for CyanoHABs. Our observations revealed that a summer bloom in Grand Lake St. Marys was initiated with *Dolichospermum* and then shifted to *Planktothrix* dominance. This transition was associated with nitrogen metabolism genes, suggesting that nitrogen plays a key role in bloom persistence through interactions among nitrogen-fixing bacteria, ammonia-oxidizing archaea, anammox bacteria, and denitrifiers. Additionally, metagenomic data revealed a strong positive correlation of toxin concentration with carbohydrate-nitrogen-sulfur-fatty acid associated metabolic pathways and a strong negative correlation with pollutant degradation pathways. Intriguingly, diazotrophic methane-related microbes were detected, which opens discussion on potential symbiosis that couples nitrogen and carbon metabolism. Toxin-degrading bacteria, such as *Polynucleobacter* and *Acidovorax*, were positively correlated with fungi like *Vishniacozyma*, proposing their cooperative roles during bloom events. Notably, *Rhodobacter*, a photosynthetic purple non-sulfur bacterium, showed strong negative correlations with both *Planktothrix* and the toxin-producing gene *mcyE*, positioning it as a promising biomarker for early bloom detection. Overall, this study advances the understanding of *Planktothrix*-dominated bloom ecology and highlights microbial signatures for proactive CyanoHAB management in freshwater systems.

1. Introduction

The occurrence of cyanobacterial harmful algal blooms (CyanoHABs)[1] is increasing in frequency and duration worldwide (Huisman et al., 2018; Paerl et al., 2011). Freshwater cyanobacterial blooms threaten drinking water supplies and recreational activity, causing significant negative impact in local and regional economies (Cheung et al., 2013; Mishra, 2023; Otten and Paerl, 2015). Various cyanobacterial genera, including *Microcystis, Planktothrix, Dolichospermum* (formally *Anabaena*), *Aphanizomenon*, and *Cylindrospermopsis* are known to cause

* Corresponding author.
E-mail address: daewook.kang@utoledo.edu (D.-W. Kang).

[1] Abbreviations: Anammox, Anaerobic ammonium-oxidizing bacteria; °C, Degree centigrade/Celsius; CyanoHABs, Cyanobacterial harmful algal blooms; DMSO, Dimethylsulfoxide; DN, Dissolved nitrogen; DOC, Dissolved organic carbon; DP, Dissolved phosphorus; ELISA, Enzyme Linked Immunosorbent Assay; GLSM, Grand Lake St. Marys; GFF, Glass fiber filter; ITS, Internal transcribed spacer; KEGG, KyotoEncyclopedia of Genes and Genomes; KO, KEGG Orthology; L, Liter; μM, Micro mole; MC, Microcystin; mL, Milli liter; min, minute; N, Nitrogen; OTUs, Operational taxonomic units; P, Phosphorus; PN, Particulate nitrogen; PP, Particulate phosphorus; qPCR, Quantitative real-time Polymerase Chain Reaction; rDNA, rRNA gene; sec, second; TN, Total nitrogen; TP, Total phosphorus.

https://doi.org/10.1016/j.watres.2025.123683
Received 31 December 2024; Received in revised form 31 March 2025; Accepted 18 April 2025
Available online 28 April 2025
0043-1354/© 2025 The Authors. Published by Elsevier Ltd. This is an open access article under the CC BY license (http://creativecommons.org/licenses/by/4.0/).

blooms in freshwater and produce toxins (Carmichael, 2001; Foysal et al., 2024). Among these, *Planktothrix* is of particular concern due to its relatively greater resilience compared to other cyanobacterial species (Kurmayer et al., 2016; Viaggiu et al., 2004). Its adaptability and persistence pose an increasing threat to freshwater ecosystems and water management strategies globally (Foysal et al., 2024; Toporowska et al., 2020).

Planktothrix is a non-nitrogen-fixing filamentous cyanobacterium (McKindles et al., 2022) that forms dense surface bloom in temperate lakes (Briand et al., 2008). Unlike *Microcystis* which tends to form surface scums, *Planktothrix* thrives at greater depths, creating blooms that are less visible but still present significant risks to aquatic environments and water quality. Together with phosphorus, inorganic nitrogen is a key nutrient that influences the growth, proliferation, and toxin production by *Planktothrix* (Gobler et al., 2016). Its ability to uptake and store nitrogen through synthesizing cyanophycin granules has been known to give *Planktothrix* an advantage during nitrogen-deficient period (Hampel et al., 2019; McKindles et al., 2022). Buoyancy, light-harvesting capacity, shade tolerance, and physiological adaptation capabilities also enable it to dominate throughout the water column (Kurmayer et al., 2016). Additionally, *Planktothrix* produces secondary metabolites, including hepatotoxic heptapeptide microcystins (Kurmayer et al., 2015) and protease inhibitors (McKindles et al., 2022), which may act as chemical defenses against antagonistic microbes, influencing surrounding aquatic biota and thereby shaping the bloom niche (Kurmayer et al., 2016).

Previous studies have explored various factors affecting *Planktothrix*-dominated blooms, including neighboring microbial diversity, physicochemical conditions, and parasitic-predatory interactions (Briand et al., 2008; Zhang et al., 2021). Wagner et al. (2023) explored interactions with parasitic fungi or cyanophages highlighting biotic influences. Steffen et al. (2012) employed metagenomics to study environmental factors and nitrogen assimilation genes driving bloom, while studies on genome variations examined differences in carbon, nitrogen, and sulfur metabolism across *Planktothrix* strains (Zhang et al., 2020). Nutrient acquisition and metabolic pathways related to *Planktothrix* have also been explored using genomic and qPCR analyses (McKindles et al., 2021b, 2022). While valuable, these studies are limited to brief seasonal or monthly timescales and focus on cyanobacterial shifts driven by abiotic factors (Zhang et al., 2021) rather than the broader microbiome that underpins and sustains these blooms. A comprehensive understanding of the entire microbiome, particularly the phycosphere surrounding *Planktothrix* blooms, remains largely unexplored, since diverse groups of microbes (bacteria including cyanobacteria, archaea, eukaryotes, fungi, and viruses) interact through competition, synergism, and parasitism. Moreover, key microbial taxa that could act as biomarkers of bloom dynamics are understudied, despite their potential to influence bloom stability and toxin production. This gap underscores the need for a more focused investigation into the microbiome's role in supporting and sustaining cyanobacterial blooms, especially through long-term monitoring.

Accordingly, the overall objectives of this study were to (i) investigate microbial community dynamics within *Planktothrix*-dominated blooms, (ii) identify key metabolic interactions among bacterial, fungal, and archaeal communities, and (iii) discover microbial or functional biomarkers indicative of shifts in bloom dynamics. Grand Lake St. Marys (GLSM), the largest inland lake in Ohio, USA, was selected as a model ecosystem due to its history of persistent *Planktothrix* blooms (Gorham et al., 2017) and high toxin production (Filbrun et al., 2013). Thus, we hypothesized that (i) neighboring microbes will have positive and/or negative association with the bloom-forming *Planktothrix* and associated physicochemical variables, (ii) potential symbiotic and/or competitive interactions among the microbial community will be identified as targets for experimentation to further understanding the course and dynamics of the *Planktothrix* bloom, and (iii) there will be microbial and/or functional signatures available that can serve as early warning biomarkers in GLSM. Through next-generation sequencing and qPCR analyses, the current study investigated bacterial, archaeal, and fungal dynamics along with functional indicators of nutrient-driven metabolism during blooms. Additionally, microbial signatures were also identified as potential biomarkers for detecting changes in the microbial dynamics of *Planktothrix*-dominated CyanoHABs.

2. Materials and methods

2.1. Sample collection and processing

During the continuous biweekly surveillance period from May 2021 to the end of July 2022, 1 L samples were collected from Grand Lake St. Marys at the Celina water treatment plant intake, (lat/long 40.54278; −84.57139) (**Fig. S1**) in HCl-washed opaque plastic bottles. Bottles were rinsed with raw water three times. Samples were stored in ice packs and shipped overnight to the lab at the University of Toledo.

2.2. Nutrient and physicochemical parameter measurement

Water quality parameters [pH, conductivity, dissolved organic carbon (DOC), dissolved nitrogen (DN), dissolved phosphorus (DP), and total phosphorus (TP)] were measured using standard methods (EPA 365.3), total nitrogen (TN) was measured using HACH (TNT826) kit. The particulate forms of nitrogen and phosphorus (PN and PP, respectively) were calculated by subtracting the dissolved concentrations from the total concentration, reflecting the cellular portion of these nutrients. Twenty mL samples were filtered through 0.45 μm PES filters. The filtrate was used to analyze DOC and DN using a TOC analyzer (TOC-$V_{CPH/CPN}$, Shimadzu Corporation, Japan), and DP and TP were analyzed using 0.45 μm filtered and unfiltered samples followed by 1 hour of digestion at 100°C using HACH (TNT843) kit, respectively. Pigments (chlorophyll-a, dissolved phycocyanin, and total phycocyanin) were measured following filtration and extraction. Ten mL of samples were filtered through 0.45 μm glass fiber filter (GFF), and the filtrate was used to measure the dissolved phycocyanin. Twenty mL of samples were passed through 0.7 μm GFF, and the filter was stored at −80 °C in dark for preservation. Later the filter was chopped into half, and each of the halves were used for chlorophyll-a and phycocyanin extraction with DMSO and phosphate buffered saline, respectively. Protocols and methods are outlined in supplementary materials (**Supplementary Text S1**). Both pigments were quantified by using a spectrophotometer (RF-6000, Shimadzu Corporation, Japan).

2.3. Nucleic acid extraction

Two hundred and fifty mL water samples were passed through 0.2 μm cellulose nitrate membrane filters. The filters were stored at −80°C for DNA extraction. The filters were processed for microbial DNA extraction using commercially available DNA extraction kit (Qiagen Power Soil Pro Kit, ref. 47,014, Qiagen GmbH, Germany). The concentration of DNA was measured with a Nanodrop ND-1000 spectrophotometer (Thermo Scientific, USA).

2.4. Amplicon sequencing and metagenomic sequencing

Extracted DNA was sent to the Genomics facility at the Biodesign Institute in Arizona State University for sequencing through NextSeq Illumina sequencing platform. 16S rRNA gene (rDNA) and fungal internal transcribed spacer (ITS) sequencing were performed using primers 515F–806R (516F: GTGCCAGCMGCCGCGGTAA; 806R: GGACTACHVGGGTWTCTAAT) (Caporaso et al., 2011) and primers ITS1f-ITS2 (ITS1f: CTTGGTCATTTAGAGGAAGTAA and ITS2: GCTGCGTTCTTCATCGATGC) to amplify 16S rDNA V4 region and 16S-23S ITS rDNA, respectively (Smith and Peay, 2014; White et al., 1990). Following sequencing, we analyzed the 16S rRNA and fungal ITS

gene sequencing data using Quantitative Insights Into Microbial Ecology (QIIME2) (Bolyen et al., 2019). Out of a total of 3,801,953 sequence reads following quality trimming, 3,434,743 forward 16S rDNA reads were analyzed for bacterial community analysis, and 1,663,213 forward reads out of 1,869,992 fungal ITS sequences were used for fungal community analysis. Average quality scores were selected above 30 for the sequence analysis, and the Greengenes (DeSantis et al., 2006) and Unite (version 9) (Nilsson et al., 2019) classifiers were used for bacterial and fungal taxonomic annotation, respectively. Metagenomic sequences were analyzed using the HMP Unified Metabolic Analysis Network (HUMAnN3) pipeline (Beghini et al., 2021). Forward reads from the shotgun metagenomic sequences were analyzed for identification and sequential phylogenetic profiling to species level using ChocoPhlAn (Beghini et al., 2021), followed by assignment of functional level through alignment of sequences with reference databases. Bowtie2 was used for accelerated nucleotide level search, Diamond for translated searches, and the Uniref protein database for protein followed by aligning with MetaCyc (Caspi et al., 2014) for gene families and pathways. Gene and pathway abundances were normalized as copy per million for further analysis. To assess bacterial metabolism in the transition to *Planktothrix*-dominated bloom, shotgun metagenomic sequening reads were assigned to KEGG Orthology (KO) values and mapped them in Kyoto Encyclopedia of Genes and Genomes (KEGG) database (Kanehisa and Goto, 2000).

2.5. Quantitative real-time PCR (qPCR)

We diluted the DNA 1:10 to nullify the effect of inhibitory agents in the DNA elution, then performed qPCR analysis targeting the cyanobacterial 16S rRNA gene, microcystin producer (*mcyE*) gene, and microcystin degrader (*mlrA*) genes using the specific primers and probes outlined in Table 1 and methods described in supplementary materials (**Supplementary Text S2**).

2.6. Toxin extraction and analysis

The total microcystin concentration in water samples was measured at the Celina Water Treatment Plant using the Ohio EPA Microcystin-ADDA ELISA method (Ohio, 2015).

2.7. Statistical analysis, network plotting and heatmaps

Statistical analyses were performed using python (v2.7), and visualizations were created using R studio (4.2), Gephi, OriginPro, and Biorender. Spearman correlation was used in all cases of correlation and network analysis, and p values under 0.05 were accepted as significant after being corrected using the Benjamini-Hochberg protocol. Among the microbial isolates, bacterial archaeal, and fungal taxa identified up to the genus level were selected based on total relative abundance for network and heatmap creation.

3. Results and discussion

3.1. Monitoring chlorophyll-a and phycocyanin dynamics

From May 2021 to July 2022, we conducted bi-weekly surveillance in GLSM to analyze chlorophyll-a and phycocyanin pigment levels, representing phytoplankton (algae and cyanobacteria, respectively). While Zepernick et al. (2024) highlighted the challenges of defining a bloom under varying aquatic condition, we adopted a standard criterion recommended by the Ohio Environmental Protection Agency (Ohio EPA) to classify bloom severity based on chlorophyll-a concentration. According to this criterion, a minor bloom is defined when chlorophyll-a levels are between 2 and 5 μg/L, a moderate bloom when levels range from 5 to 50 μg/L, and a severe bloom when chlorophyll-a exceeds 50 μg/L (Dewine and Stevenson, 2020). During the surveillance period, a continuous bloom was observed, except on 09/07/2021, based on the bloom criteria set by the Ohio EPA (Dewine and Stevenson, 2020) (Fig. 1**A**). The bloom reached moderate intensity (5–50 μg/L chlorophyll-a) for a large portion of the surveillance period (13 out of 33 occasions). It frequently progressed to high intensity (>50 μg/L chlorophyll-a) on 13 out of 33 occasions. This unceasing bloom in GLSM throughout the seasons has been extensively documented since 2011 (Dumouchelle and Stelzer, 2014), while the evidence of water quality deterioration and cyanobacterial dominance was recorded even earlier in 1970s (Filbrun et al., 2013; Jacquemin et al., 2023). There was a strong and significant correlation between chlorophyll-a and the total phycocyanin concentration ($r = 0.94$, $p < 0.001$), indicating the bloom in GLSM was primarily driven by cyanobacteria rather than eukaryotic algae (Berry et al., 2017). Meanwhile, we observed a spike in dissolved phycocyanin levels on 7/13/2021 (up to 250 μg/L in Fig. 1**A**), suggesting the possibility of cell lysis and the release of intracellular material from cyanobacteria.

Throughout the period, we also monitored cyanobacterial toxin levels using ELISA. The total microcystin concentration was found in the range from < 0.3 μg/L to 23.8 μg/L (Fig. 1**B**) and was significantly correlated with the level of cyanobacterial pigments: total phycocyanin ($r = 0.56$, $p < 0.001$) and chlorophyll-a ($r = 0.57$, $p < 0.001$). The total microcystin concentration also showed a positive correlation with the absolute amount of the *mcyE*, a gene encoding an enzymatic step in microcystin biosynthesis ($r = 0.51$, $p = 0.0025$). The amount of the *mcyE* gene exhibited a similar pattern to that of the cyanobacterial 16S rRNA gene (*16S_Cyn)* abundance quantified by qPCR (Fig. 1**C**). The *mlrA* gene, responsible for degrading microcystin, followed a trend similar to the measured microcystin concentrations (Fig. 1**B, C**). The physical and water quality parameters of lake water were also monitored to understand their contribution to the bloom in GLSM (**Table S1** and **Fig. S2**). TP ranged from 0.034 mg/L to 0.699 mg/L, DN varied from 0.16 mg/L to 3.50 mg/L, and DOC varied from 5.0 mg/L to 19.3 mg/L (**Fig. S2**). Historically, GLSM has been hypereutrophic, with a record of external nutrient input (both nitrogen and phosphorus) (Filbrun et al., 2013; Steffen et al., 2014) and we also observed a TP concentration > 0.1 mg/L (0.7 mg/L on average) throughout the study period.

Table 1
qPCR primers and probes for target gene analysis.

Target Group	Oligonucleotides	Sequences (5′–3′)	Ref.
*16S_Cyn**	16SF	AGCCACACTGGGACTGAGACA	(Al-Tebrineh et al., 2010)
	16SR	TCGCCCATTGCGGAAA	
	16SP	**FAM-**CCTACGGGAGGCAGCAGTGGG**-BHQ1**	
mcyE/ndaF	mcyF + flap	AATAAATCATAATTTAGAACSGGVGATTTAGG	(Al-Tebrineh et al., 2012)
	mcyR + flap	AATAAATCATAACGRBTVADTTGRTATTCAATTTCT	
	mcyP	**FAM-**AATCAAGTTAAGGTVAATGGYTATCG**-BHQ1**	
mlrA	F-primer	AGCCCKGGCCCRCTGC	(Hoefel et al., 2009)
	R-primer	ATGCCARGCCCACCACAT	
	Probe	**FAM-**TGCCSCAGCTSCTCAAGAAGTTTG**-BHQ1**	

* cyanobacterial 16S rRNA gene.

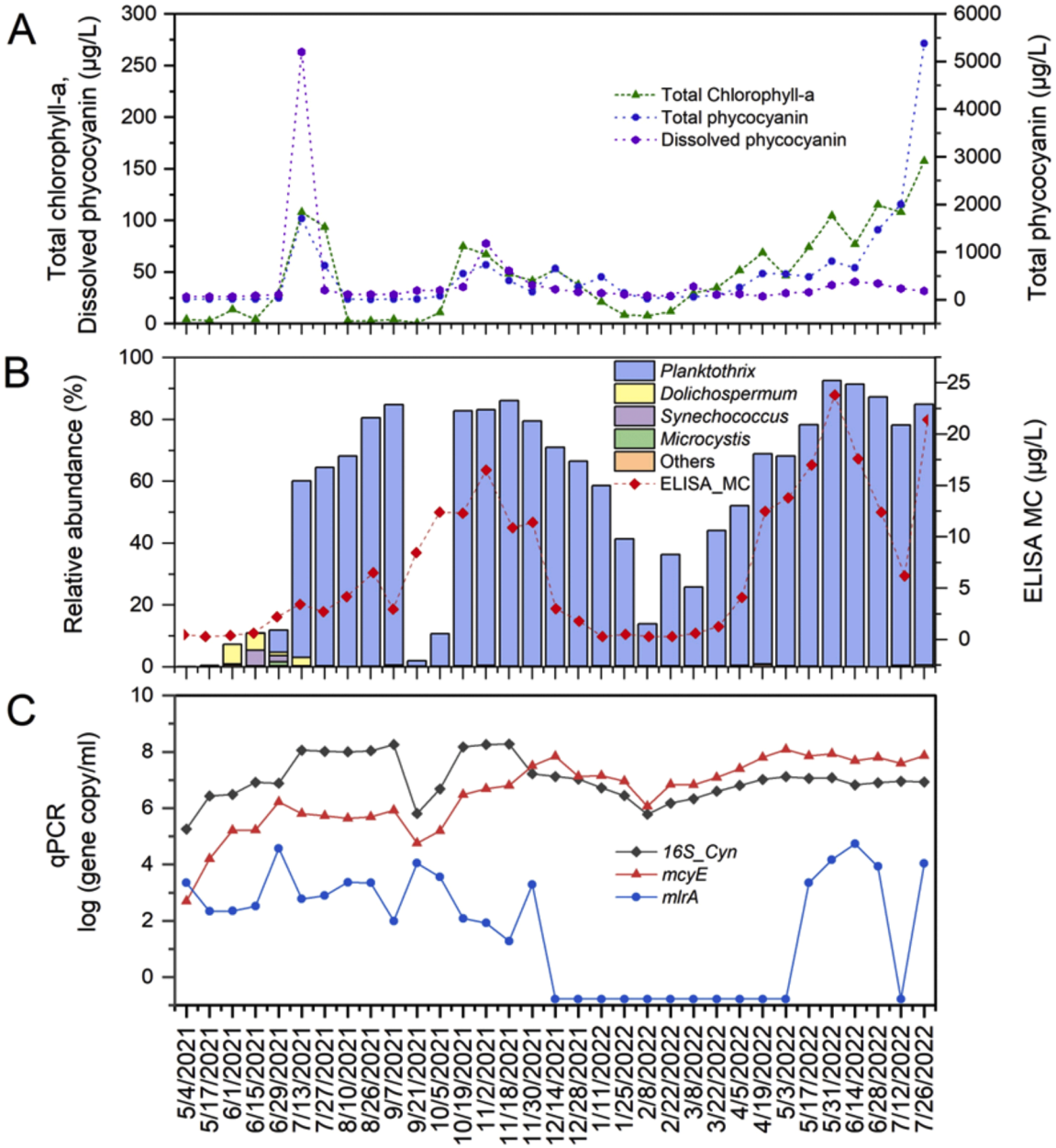

Fig. 1. Bloom observation using temporal dynamics of pigments, cyanobacterial species, and target genes. Changes in (A) pigment levels of total/dissolved phycocyanin and total chlorophyll-a, (B) the abundances of cyanobacterial species measured by 16S rRNA gene sequencing and quantitative real-time PCR (qPCR) targeting cyanobacterial species through years 2021–2022 in Grand Lake St. Marys, and (C) a graphical trend of microcystin (ELISA_MC) concentration with the level of cyanobacterial 16S rRNA, *mcyE*, and *mlrA* genes by qPCR (unit: log gene copy/ml).

3.2. Initial bloom of Dolichospermum transitioning to Planktothrix

We first investigated the dynamics of the cyanobacterial blooms in GLSM by 16S rRNA gene amplicon sequencing analysis. During the sampling period, a total of 1,030 operational taxonomic units (OTUs) were observed, with 34 OTUs classified into 18 different cyanobacteria at the genus level. In 2021, the cyanobacterial bloom started with *Dolichospermum* (the relative abundance based on 16S rRNA amplicons, 6.4 %) on 06/01/2021. Its relative abundance was relatively low, but the bloom was severe based on an absolute amount of cyanobacteria by qPCR ($>10^5$ gene copies per mL, a severe bloom according to Ohio EPA (Dewine and Stevenson, 2020)). It is unexpected to observe that non-*Planktothrix* cyanobacteria initiated the bloom, as *Planktothrix* has been the dominant cyanobacterial species reported in GLSM over the last decade (Jacquemin et al., 2023). *Planktothrix* was the only dominant cyanobacterial genus in GLSM, since Steffen et al. (2014) reported a switch between *Planktothrix* and *Microcystis* in 2010. After a brief coexistence of *Dolichospermum* (5.4 %) and *Synechococcus* (5.1 %) on 06/15/2021, *Planktothrix* (7.2 %) emerged on 06/29/2021 and gained dominance within two weeks (up to 57.1 %) on 07/13/2021, outnumbering *Synechococcus* (2.0 %) and *Dolichospermum* (1.0 %) (Fig. 1**B**). The *Planktothrix* bloom persisted in GLSM for most weeks, with intermittent declines in fall 2021 (late September to early October) and winter 2022 (early February) (Fig. 1**B**). The relative abundance of *Planktothrix* was significantly correlated with the absolute abundance of cyanobacteria measured by qPCR ($r = 0.71$, $p < 0.001$), confirming the quantitative dominance of *Planktothrix* in the bloom. The dominance is also supported by its strong positive correlations with all pigments: total chlorophyll-a ($r = 0.59$, $p < 0.001$), total phycocyanin ($r = 0.58$, $p < 0.001$), and dissolved phycocyanin ($r = 0.61$, $p < 0.001$) (Fig. 2**A**).

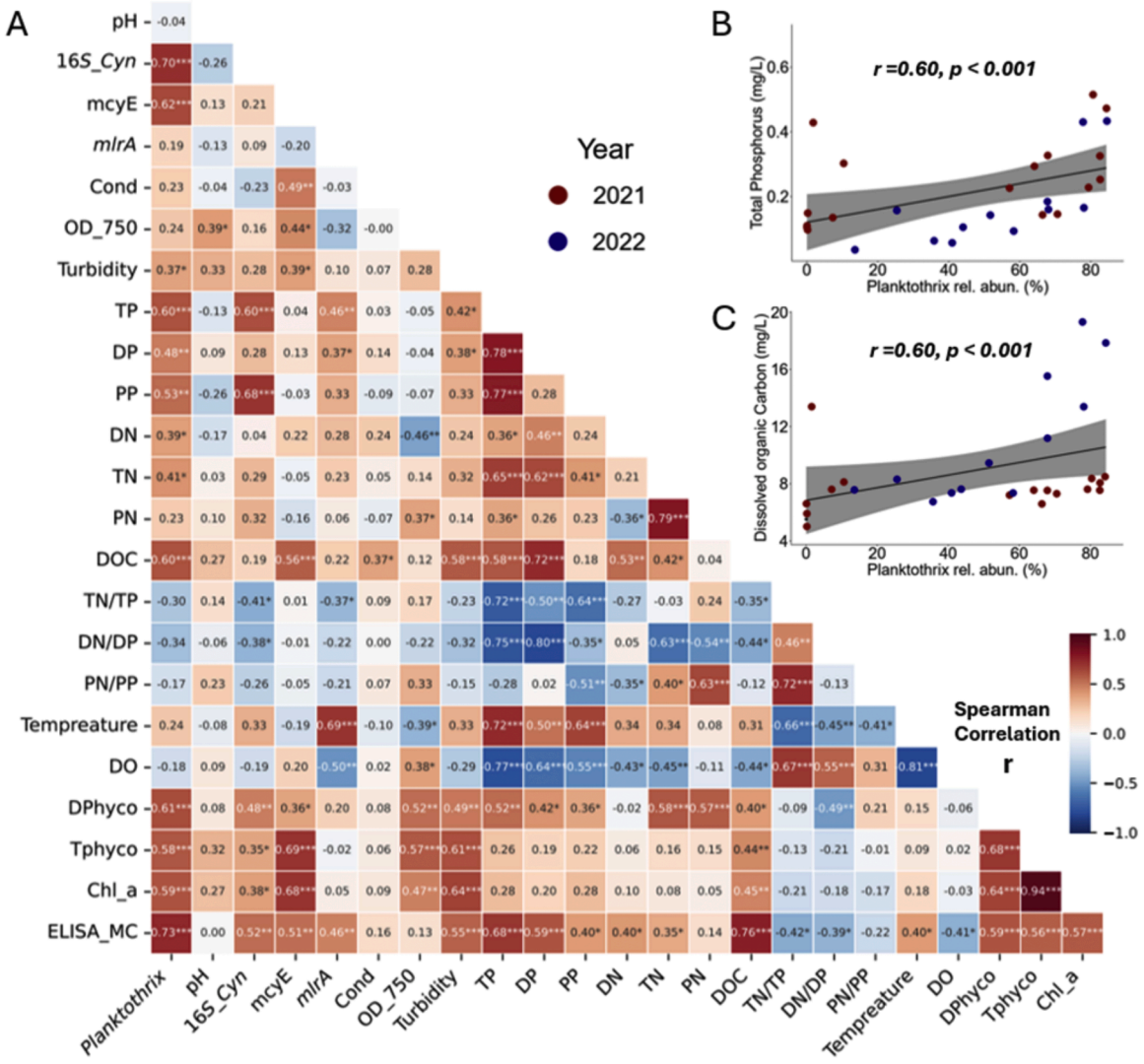

Fig. 2. Correlation analysis of *Planktothrix* relative abundance with water quality parameters and key genes. (A) Correlogram of *Planktothrix* relative abundance, between the water parameters and several genes of interest, (B) correlation between *Planktothrix* and total phosphorus concentration and (C) correlation between *Planktothrix* and dissolved organic carbon concentration.

Interestingly, there was an initial spike in dissolved phycocyanin levels at the onset of the *Planktothrix* bloom on 7/13/2021 (Fig. 1**B**). The second major peak in dissolved phycocyanin was followed on 11/2/2021, coinciding with the beginning of the second wave of the *Planktothrix* bloom. These abrupt increases in dissolved phycocyanin levels may reflect a consequence of competitive dynamics when *Planktothrix* gained dominance against neighboring microbes. Metagenomic sequencing analysis also confirmed the dominance of *Planktothrix* at the species level, revealing *Planktothrix agardii* was the most abundant (89 %) followed by *Planktothrix rubescens* (8 %) (**Fig. S3**). This observation is consistent with previous findings that identified *P. agardii* as the most predominant species in GLSM (Schmidt et al., 2013; Wagner et al., 2023). Ecologically, *P. agardii* has been categorized as the codon S1 that thrives in turbid, mixed, and light-deficient environments (Padisák et al., 2009; Reynolds et al., 2002), characteristics that align well with the conditions of shallow GLSM. Thus, the ecophysiology and cyanobacterial interactions in GLSM appear to be primarily driven by *P. agardii*.

The transition from a *Dolichospermum* to a *Planktothrix* bloom after 06/29/2021 could be attributed to changes in environmental conditions and/or nutrient availability (Reinl et al., 2023; Zhang et al., 2021). First, we observed a sudden increase in temperature on 06/29/2021 (**Fig. S2D**), coinciding with an increase in the relative abundance of *Planktothrix*. In late fall 2021, the relative abundance of *Planktothrix* decreased and then returned in spring 2022, along with increases in water temperature. An increase in turbidity levels in June 2021 (**Fig. S2C**) also corresponded to the emergence of *Planktothrix*, and its relative abundance was found to have a significant correlation with turbidity (Fig. 2**A**, $r = 0.37$, $p = 0.03$). *Planktothrix* sp. (e.g., *P. agardhii* and *P. rubescens)* are known to thrive under self-shading conditions, leading to an increase in turbidity and perennial blooms in eutrophic and hypereutrophic conditions (Kurmayer et al., 2016; Rücker et al., 1997). In addition, nutrient availability may explain the switch from a *Dolichospermum* to a *Planktothrix* bloom. *Planktothrix* was positively correlated with nutrient levels of TP ($r = 0.60$, $p < 0.001$) and DOC ($r = 0.60$, $p < 0.001$). Its correlation with nitrogen levels were relatively weak (DN, $r = 0.39$, $p < 0.05$; TN, $r = 0.41$, $p < 0.05$) but significant. The *Dolichospermum* bloom was followed by a decrease of DN:DP and TN:TP ratio on 05/17/2021 (**Fig. S2L-M**). The DN:DP ratio captures short-term bioavailable nutrient conditions in surrounding environment of cells and often aligns with bloom toxicity patterns, especially when phosphorus becomes limiting (Chaffin and Bridgeman, 2014; Ma et al., 2015). Whereas, the TN:TP ratio is the most widely applicable and integrative metric for evaluating nutrient limitation in eutrophic

systems. It reflects long-term nutrient loads and correlates with cyanobacterial dominance, particularly when the TN:TP falls below critical thresholds—commonly <16:1 atomic or <29:1 by weight (Howarth et al., 1988; Paerl et al., 2001; Smith, 1983). Therefore, the low DN:DP and TN:TP conditions both falling below around 20 by mass ratio (**Fig. S2L, M**) indicate nitrogen limitation and favors the growth of a nitrogen-fixing cyanobacterium like *Dolichospermum* (Moisander et al., 2003). Fixed nitrogen, such as ammonia, could be released and available for *Planktothrix* during its initial emergence in June in response to increased dissolved and total phosphorus levels (**Fig. S2J, K**), since *Planktothrix* has been shown to be an effective scavenger of ammonium (Hampel et al., 2019). Then, the growth of *Planktothrix* was enhanced when additional external nitrogen became available in August 2021 (**Fig. S2H, I**). Similarly, the growth of nitrogen-fixing cyanobacteria preceding non-nitrogen-fixing cyanobacterial blooms has been reported in other lake systems. Wang et al. (2021) observed that nitrogen-fixing cyanobacteria initiated a bloom in Lake Harsha, while nitrogen levels were still high. This was followed by a bloom of non-nitrogen-fixing species like *Microcystis* and *Planktothrix* during nitrogen limitation. Beversdorf et al. (2013) also demonstrated how nitrogen limitation favors nitrogen-fixing cyanobacteria.

3.3. Metabolic pathways and role of nitrogen metabolism in bloom progression and toxicity

Nutrient and cyanobacterial dynamics discussed above suggest that nitrogen-fixing cyanobacteria possibly contributed to the growth and dominance of *Planktothrix*. To assess how nitrogen metabolism might be involved in the transition to a *Planktothrix*-dominated bloom, shotgun metagenomic sequence analysis was performed as described in the Materials and methods section. When the sequence reads were assigned to KO values and mapped in KEGG, two ammonia-producing enzymes, nitrogenase and nitrilase, were found to be abundant right before and at the time *Planktothrix* emerged as the dominant cyanobacterial species on 7/13/2021 (Fig. 3). Nitrogenase is the enzyme responsible for nitrogen fixation to ammonia (Fig. 3**A**), and the genes associated with nitrogenase were found in *Anabaena, Aphanizomenon, Cylindrospermopsis, Dolichospermum*, and *Limnohabitans* (Fig. 3**C**) and in both *Aphanizomenon* and *Dolichospermum* at the gene level (**Fig. S5**). The enzyme nitrilase converts nitrile to ammonia (Fig. 3**C**), and our metagenomic analysis

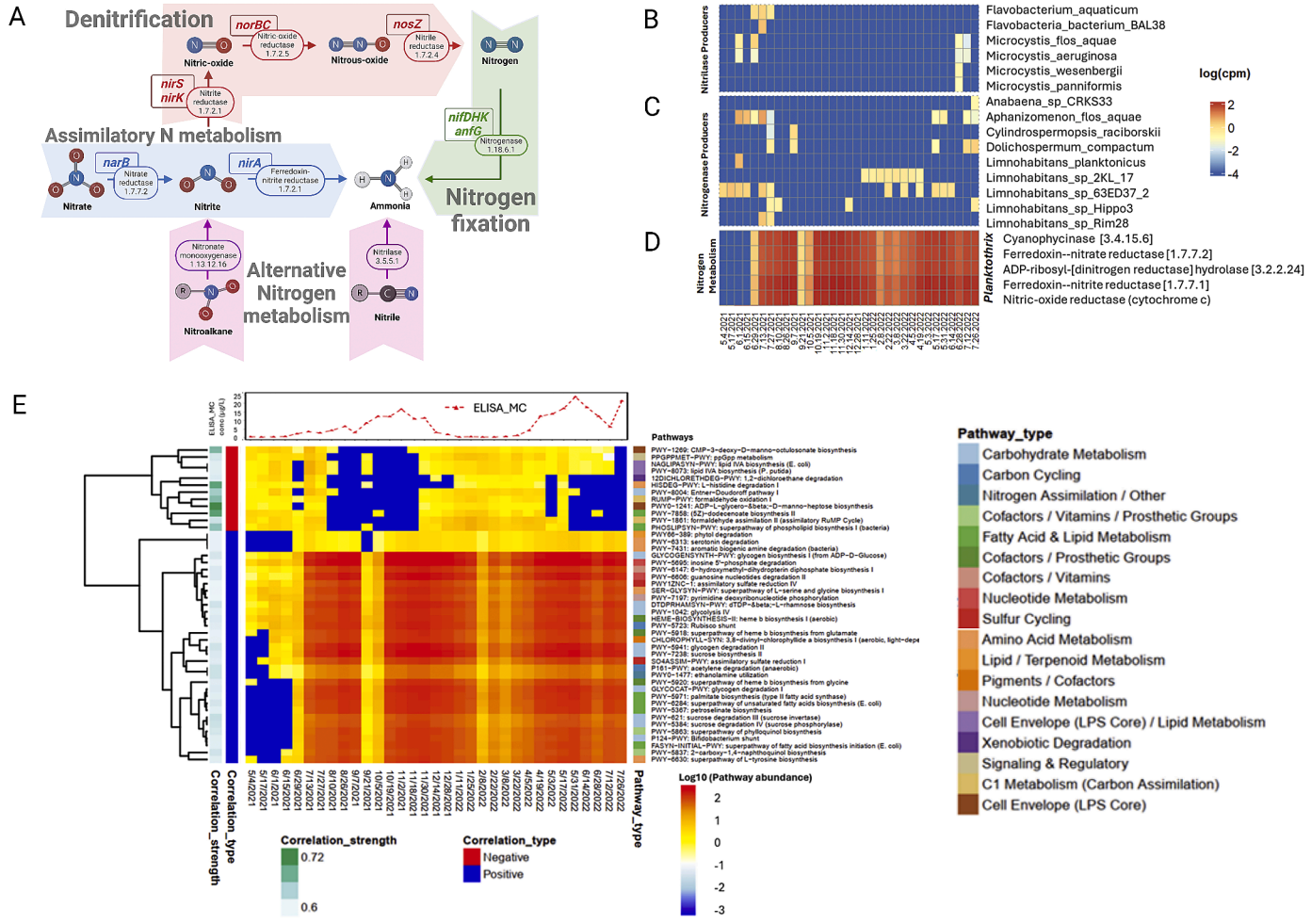

Fig. 3. Outline of nitrogen metabolism, metabolic pathways relating to nitrogen metabolism and pathways relating toxin concentration- identified through metagenomic sequencing. KEGG pathway showing the assimilatory nitrogen metabolism (performed by enzymes 1.7.7.1 and 1.7.7.2) which were found strongly associated with *Planktothrix* relative abundance caused the dominance of *Planktothrix* bloom in GLSM: (A) the nitrogen metabolism pathways and contributing enzymes, EC numbers and respective genes coding those enzymes. Green arrow indicates nitrogen fixation whereas the sky-blue color indicates assimilatory nitrogen metabolism by *Planktothrix,* purple color indicates nitrilase or alternative nitrogen metabolism activities, and red color indicates denitrification, (B) heatmap of nitrogenase gene producers abundance, (C) heatmap of nitrilase producing gene abundance in different species, (D) heatmap of gene abundance of nitrogen metabolism related genes in *Planktothrix*. Units are shown in log gene copies per million (CPM) units. (E) Time series line plot showing cyanotoxin concentrations (ELISA_MC) in GLSM integrated with heatmap showing top 46 bacterial pathways having significant correlation ($|r| > 0.58$ and $q < 0.002$ through Spearman correlation analysis) with ELISA_MC. Here, the legend colors indicate correlation types and pathway types.

suggested that *Flavobacterium, Flavobacteria,* and *Microcystis* contained the genes associated with nitrilase (Fig. 3**B**). When genes for nitrogenase and nitrilase were abundant, the abundance of *Planktothrix* genes associated with assimilatory nitrate reduction and denitrification increased (Fig. 3**D**). Although further transcriptomic analysis is essential to confirm it, *Planktothrix* may potentially have responded to the availability of nitrogen via nitrate reductase, denitrogen reductase, ferredoxin-nitrite redutase, and nitric-oxide reductase (Fig. 3**D**). In addition, the cyanophycinase enzyme-coding gene (Fig. 3D) was detected in *Planktothrix*, implying the capability of utilizing cyanophycin as the nitrogen reserve compound. In a previous study (Hampel et al., 2019), expression of the cyanphycinase gene was reported during nitrogen-limited periods. *Planktothrix*, a non-diazotrophic cyanobacteria, may take advantage of the nitrogen fixation by diazotrophic cyanobacterial groups, subsequently outcompeting them when external nitrogen is available in GLSM.

Cyanobacterial proliferation depends on phosphorus and nitrogen levels (Barnard et al., 2021; Ferber et al., 2004; Gobler et al., 2016), with ongoing discussions regarding whether one or both nutrients are limiting factors for their growth, diversity, and toxin production. The nitrogen to phosphorus (N:P) molar ratio often serves as a measure to assess the nutrient status and limitation (Paerl et al., 2001), which may drive both bloom formation and toxin production (Wagner et al., 2021). We found that the abundance of nitrogen-fixing gene was concomitant with a decrease of the DN:DP ratio (**Fig. S2L**) but not much related with the PN:PP ratio (**Fig. S2M**). While the PN:PP ratio often indicates nutrient limitation within algal cells, Ma et al. (2015) emphasized the DN:DP ratio as a better indicator of nutrient availability. This is because only dissolved forms of nitrogen and phosphorus are readily accessible to phytoplankton, not the particulate forms. Regarding toxin levels, positive correlations were observed with individual DP and DN levels ($p < 0.05$), but toxin levels were negatively correlated with the DN:DP and TN:TP ratios ($r = -0.39$ and -0.42, respectively; $p < 0.05$) but not with the PN:PP ratio ($p > 0.05$) as shown in Fig. 2. Typically, higher nitrogen levels are associated with higher toxin levels, but our observation suggests that toxin production by *Planktothrix agardhii* could be more closely linked to phosphorus availability, especially when nitrogen is in relative excess.

To better understand the metabolic underpinnings of cyanobacterial bloom dynamics and toxin production, we conducted Spearman correlation analyses between 270 bacterial pathway abundances derived from metagenomic functional profiling and microcystin concentrations measured by ELISA (ELISA_MC in Fig. 3**E**). Among 156 microbial pathways significantly correlated with ELISA_MC ($p < 0.05$, as shown in **Fig. S4**), the top 46 significant microbial pathways ($|r| > 0.58$, $q < 0.002$) encompass core metabolic functions such as carbohydrate metabolism, nitrogen assimilation, sulfur cycling, amino acid and lipid biosynthesis, and detoxification processes (Fig. 3**E** and **Table S2)**. First, carbohydrate metabolism was prominently represented among positively correlated pathways, including glycolysis IV (PWY-1042), glycogen biosynthesis I (GLYCOGENSYNTH-PWY), sucrose degradation (PWY-621), and the Rubisco shunt (PWY-5723). These functions may support enhanced carbon flux during bloom events, providing energy and biosynthetic precursors for the rapid growth of cyanobacteria and their toxin production. Previous studies have shown that *Planktothrix agardhii* and other bloom-forming cyanobacteria possess highly efficient carbon fixation systems and central metabolic pathways—including the Calvin-Benson-Bassham cycle and carbonic anhydrases—which enable them to thrive under varying CO_2 conditions (McKindles et al., 2022; Zhang et al., 2020). These pathways also serve as metabolic branch points, channeling intermediates into secondary metabolism through the shikimate, methylerythritol phosphate (MEP), and tricarboxylic acid (TCA)-linked biosynthetic pathways that is known to drive the production of microcystin and other peptide toxins (Babele et al., 2023).

Nitrogen-related pathways, such as ethanolamine utilization (PWY0–1477) and pyrimidine deoxyribonucleotide phosphorylation (PWY-7197), were also part of the cluster containing pathways that were positively correlated with microcystin levels (Fig. 3**E**). These pathways likely represent adaptive strategies employed by bloom-forming cyanobacteria to exploit organic nitrogen sources when nitrate is limited, since ethanolamine and polyamines were utilized as nitrogen sources with the nitrogen stress and assimilation genes (such as *glnA, relA, spoT*, and *phoX*) expressed in situ under nutrient-limited conditions (Krysenko and Wohlleben, 2022; Li et al., 2023). This metabolic flexibility and ability to utilize diverse nitrogen sources—including ethanolamine, polyamines, and internally stored nitrogen may facilitate bloom intensification even under low dissolved inorganic nitrogen conditions, commonly associated with elevated microcystin levels (Beversdorf et al., 2013; Li et al., 2023; Krysenko and Wohlleben, 2022).

Sulfur metabolism, particularly assimilatory sulfate reduction (SO4ASSIM-PWY), was significantly enriched during bloom peaks (Fig. 3E). This pathway synthesizes sulfur-containing amino acids (cysteine and methionine) and detoxification cofactors like glutathione, which are vital for maintain cellular redox balance and oxidative stress tolerance in cyanobacterial blooms (Babele et al., 2023; Kharwar and Mishra, 2023; Takahashi et al., 2011; Zhang et al., 2020). Enhanced sulfur-related activity supports adaptation to nutrient limitation and stress, conditions linked to increased microcystin production in bloom-forming cyanobacteria including *Planktothrix* (Kurmayer et al., 2016; McKindles et al., 2022). Lipid and amino acid biosynthesis pathways—including palmitate biosynthesis (PWY-5971), fatty acid biosynthesis initiation (FASYN-INITIAL-PWY), and dTDP-l-rhamnose biosynthesis (DTDPRHAMSYN-PWY)—were also strongly correlated with microcystin concentrations (Fig. 3**E**). These pathways support membrane remodeling, energy storage, cellular integrity, and production of extracellular polymeric substances (EPS), facilitating bloom persistence, and stress tolerance (Babele et al., 2023; Kahn et al., 2023; Ren et al., 2024; Wang et al., 2022).

In contrast, pathways associated with detoxification, envelope biosynthesis, and organic pollutant degradation were negatively correlated with ELISA_MC (Fig. 3**E**). These include lipid A biosynthesis (NAGLIPASYN-PWY), formaldehyde assimilation (RUMP-PWY), and CMP-3-deoxy-d-manno-octulosonate biosynthesis (PWY-1260). The suppression of lipid A and CMP-KDO biosynthesis pathways suggests compromised membrane integrity and cell viability in Gram-negative bacteria such as *Limnohabitans* during blooms (Kasalický et al., 2013). Similarly, decreased formaldehyde assimilation via the RuMP pathway in *Candidatus Methylopumilus planktonicus* indicates reduced capability for organic pollutant degradation and carbon cycling (Salcher et al., 2015). Such metabolic inhibition likely reflects competitive exclusion or toxicity from bloom-forming cyanobacteria (Briand et al., 2008). Pathways with strong correlations with ELISA_MC and *Planktothrix agardii* are outlined in **Table S2** and **S3**, respectively.

The metagenomic analysis above highlighted the metabolic interplay underlying *Planktothrix* dominance, emphasizing its potential reliance on nitrogen fixation by other cyanobacteria and subsequent nitrogen assimilation pathways under nutrient-limited conditions. Additionally, strong correlations between key microbial metabolic functions—such as carbohydrate metabolism, nitrogen and sulfur assimilation, and amino acid and lipid biosynthesis—and microcystin concentrations underscore the metabolic flexibility and adaptive strategies driving bloom intensification and toxin production. Conversely, suppression of detoxification and pollutant degradation pathways in other microbes reflects competitive pressures exerted by *Planktothrix* during bloom events.

3.4. Bacterial dynamics and potential biomarkers of Planktothrix-Bloom

Overall bacterial dynamics were further investigated to identify microbial species that were noticeable during the shift in cyanobacterial bloom. Right before the onset of the *Planktothrix* bloom, Proteobacteria was the most abundant phylum (31.2 %) followed by Bacteroidetes (23.6 %), Actinobacteria (21.9 %), and Verrucomicrobia (20.7 %)

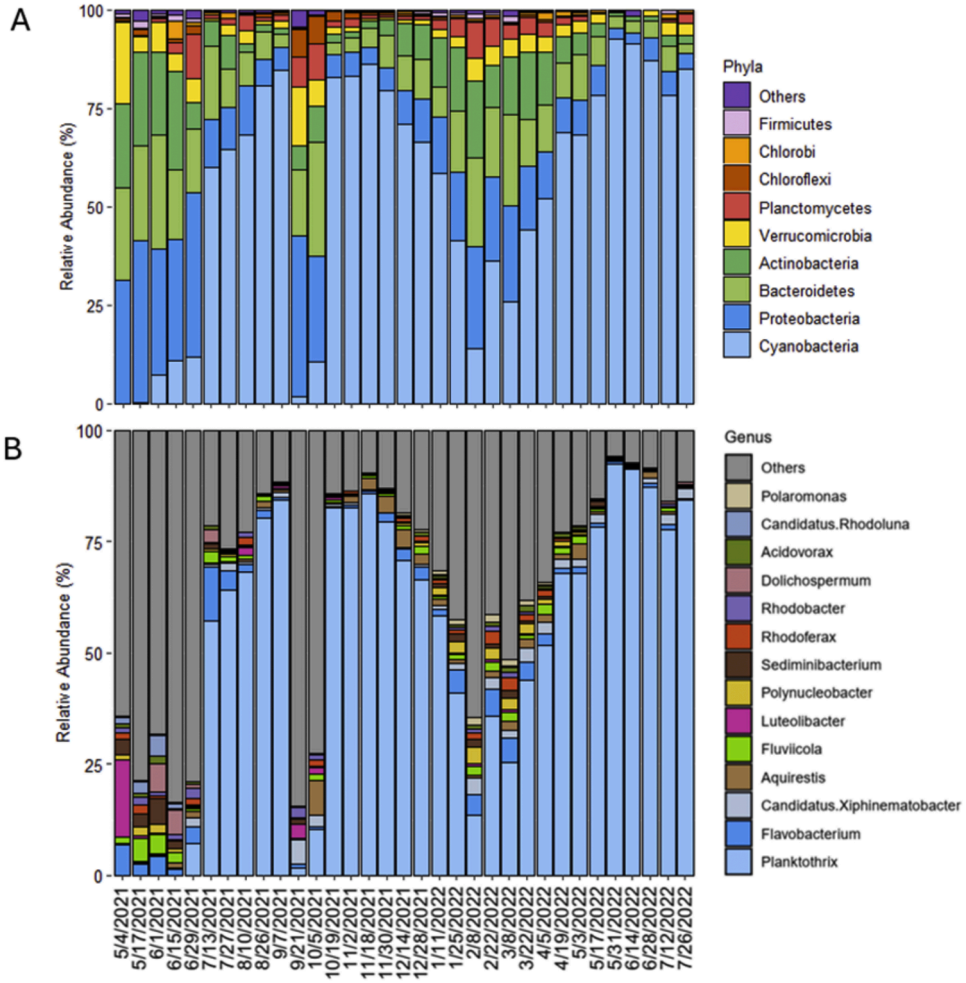

Fig. 4. Microbial community diversity changes over the time at (A) phylum and (B) genus level. Phyla having a total relative abundance over 15 % and genera having a total relative abundance over 10 % was shown in the graphs at phylum and genus level, respectively; rest of the phyla and genera were summed up and shown as others.

(Fig. 4**A**). With the progression of the bloom, the abundance of Cyanobacteria increased from 0.9 % up to 92.5 % at its highest peak. All the other major bacterial phyla showed strong negative correlations with the phylum Cyanobacteria: Proteobacteria ($r = -0.98$. $p < 0.001$), Bacteroidetes ($r = -0.93$. $p < 0.001$), Actinobacteria ($r = -0.88$. $p < 0.001$), and Verrucomicrobia ($r = -0.84$. $p < 0.001$), that suggests inverse relationship with them. At the genus level, after *Planktothrix*, the most abundant bacterial genera were *Flavobacterium, Aquirestis, Fluviicola, Sediminibacterium* (phylum Bacteroidetes), *Candidatus Xiphinematobacter, Luteolibacter* (Verrucomicrobia), and *Polynucleobacter* (Proteobacteria) (Fig. 4**B**).

A network analysis was performed to identify a potential ecological position of *Planktothrix* and its neighboring bacteria. In both 2021 and 2022, *Planktothrix* showed strong negative correlations with multiple bacterial genera, including *Sediminibacterium, Flavobacterium, Methylotenera, Acidovorax, Polynucleobacter, Fluviicola,* and *Rhodobacter* (Fig. 5**AB**). Guo et al. (2021) reported potential inhibition of cyanobacteria (*Microcystis*) by *Sediminibacterium*. However, its capability to form aggregated flocs consortia (Velichko et al., 2015) may protect cyanobacteria from opportunistic colonizers by providing microhabitat and nutrient supply (Sethuraman et al., 2022). These contradictory studies suggest the possibility of a complex relationship between *Sediminibacterium* and cyanobacteria that warrants further investigation. *Flavobacterium* is known to prey on cyanobacteria (Tromas et al., 2017). The growth of *Flavobacterium* could be facilitated by extracellular materials such as carbohydrates and biomolecules (Özbayram et al., 2020) released from cyanobacteria (Kim et al., 2020), which often appear as a symptom of the post bloom stage. *Pedobacter* was also negatively correlated with either the absolute amounts of cyanobacteria (shown as *16S_Cyn* in Fig. 5**A**) in 2021 or the relative abundance of *Planktothrix* in 2022. The algaecidal effect of *Pedobacter* (Berg et al., 2009) might lead to the increased release of cyanotoxins, potentially promoting the growth of microcystin degraders like *Methylotenera, Acidovorax*, and *Polynucleobacter* in GLSM (Massey and Yang, 2020).

Some of these bacteria listed above also showed strong negative correlations with water parameters and/or bloom indicators in 2021 ($r < -0.6$, $p < 0.05$): *Sediminibacterium* (dissolved Phycocyanin, DOC, *16S_Cyn, mcyE*, and ELISA_MC), *Flavobacterium* (TP, DOC, and ELISA_MC), and *Fluviicola* (DOC and ELISA_MC). However, none of these bacteria showed consistent associations in 2022, making them unsuitable as candidate biomarkers. Notably, however, the relative abundance of *Rhodobacter* consistently showed strong and negative correlations with *Planktothrix* and bloom indicators (the absolute amounts of *mcyE, mlrA*, and cyanobacterial 16S rRNA genes) in both 2021 and 2022 (Fig. 5). *Rhodobacter,* a purple non-sulfur phototroph, possesses the capability to degrade cyanotoxins (Pineda-Mendoza et al., 2020) and has been associated with *Microcystis* blooms in freshwater (Bagatini et al., 2014). *Rhodobacter* species are also known to accumulate phosphorus (Hiraishi et al., 1991) and fix atmospheric nitrogen (Klipp et al., 1988). Although we did not identify the genes associated with *Rhodobacter* in our metagenomic analysis, its versatile metabolic properties may give *Rhodobacter* an advantage under phosphorus and

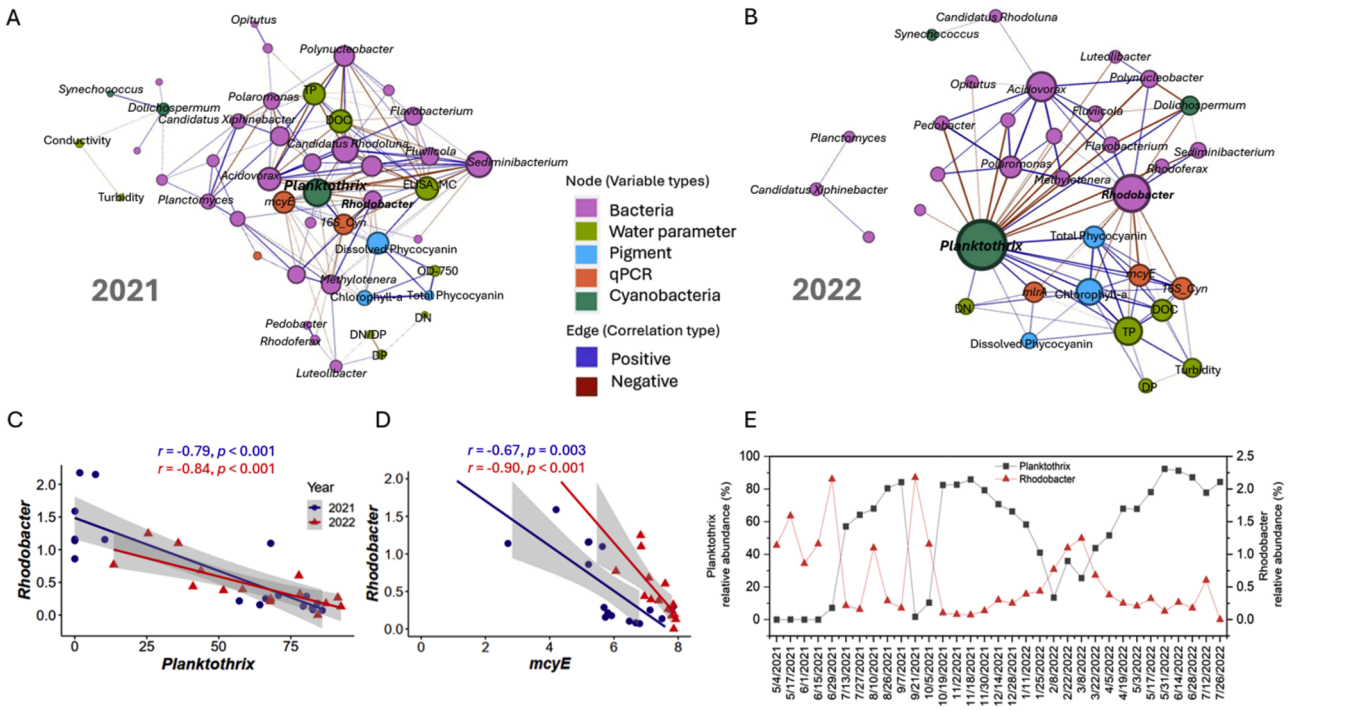

Fig. 5. Network and correlation analysis for biomarker identification. Networks among water parameters and relative abundances of significant bacterial genera in (A) 2021 and (B) 2022; Correlations of *Rhodobacter* with (C) *Planktothrix* and (D) the absolute amount of *mcyE* gene (qPCR) across 2021–2022; and (E) dynamics of *Planktothrix* and *Rhodobacter*, showing inverse growth pattern across 2021–2022.

nitrogen-limited conditions. Given the apparent inverse correlations with *Planktothrix* appeared in Fig. 5**E**, the decline in the relative abundance of the genus *Rhodobacter* could serve as a potential biomarker for the upcoming emergence of *Planktothrix*-dominating CyanoHABs.

3.5. Fungal and archaeal dynamics along with cyanobacteria

Fungi are essential counterparts to bacteria in aquatic habitats, either through mutualistic or parasitic interactions (Laezza et al., 2022). Although less studied than neighboring bacteria, the ecological position of fungi in CyanoHABs has garnered increasing attention due to the potential antifungal properties of cyanobacteria or parasitic relationships with cyanobacteria (McKindles et al., 2021a). By sequencing ITS rRNA genes, we identified 350 fungi at the genus level across all 33 samples. To explore potential symbiosis and competition in GLSM, a time series heatmap and a co-occurrence network were generated with the most abundant bacterial ($n = 30$), fungal ($n = 30$), and archaeal ($n = 9$) genera (Fig. 6**AB**). Two major clusters of fungi were observed, centered around the genera *Lachum* (Cluster 2) and *Vishiniacozyma* (Cluster 4, Fig. 6**A**). Intriguingly, *Dolichospermum* showed significant and strong negative correlations with *Lachnum* ($r = -0.67$, $p < 0.001$) and *Vishniacozyma* ($r = -0.71$, $p < 0.001$), whereas no fungal genera were significantly correlated with *Planktothrix*. Compared to *Planktothrix, Dolichospermum* might be more susceptible to a group of fungi, as species-specific fungal interactions with cyanobacteria can vary depending on the particular fungus involved (do Amaral et al., 2023). According to the network analysis (Fig. 6**B**), *Vishniacozyma* might have a mutualistic ecological position in GLSM, as it served as a hub between cyanotoxin-degrading bacteria (*Polynucleobacter, Acidovorax*, and *Polaromonas*) and the epicenter of the fungal network. *Vishniacozyma*, a psychrophilic fungi, may also have ecological advantages in winter (Perini et al., 2019) and may contribute to EPS production (Rusinova-Videva et al., 2022) and phosphate solubilization (da Silva et al., 2022), enhancing nutrient availability for surrounding microbes. The algaecidal bacterium *Pedobacter* was also positioned between *Planktothrix* and cyanotoxin-degrading bacteria (Fig. 6**B**). Fungi might benefit from the lysis of cyanobacteria by algaecidal bacteria, and the degradation of toxins may provide fungi with additional sources of nutrient, such as nitrogen or carbon. In fact, previous studies reported that fungi often thrive during the decline of cyanobacterial blooms, decomposing cyanobacterial cell components (Zhou et al., 2018). Meanwhile, in previous studies on GLSM, fungal *Rhizophydium* sp. (phylum Chytridiomycota) was shown to infect *Planktothrix* (McKindles et al., 2021b; Wagner et al., 2023). Although it was detected only once on 06/01/2021, fungal parasite chytrids (phylum Chytridimycota) were detected in 27 occasions of sampling out of 33 occasions. Although chytrids did not show a strong correlation with the relative abundance of *Planktothrix* in this study, they may still have a role in the community through predation on cyanobacteria.

Interestingly, archaea and several other bacteria associated with nitrogen and carbon cycles were identified in GLSM and clustered together in the heatmap and/or network (Fig. 6**A** and 6**B**, respectively). As shown in Cluster 1 (Fig. 6**A**), methane-producing archaea (*Methanosaeta, Methanolinea, Methanobacterium, Methanospirillum, Methanocorpusculum*, and *Methanosarcina*) and ammonia-oxidizing archaea (*Candidatus nitrososphaera*) were present in spring and early summer. Methane-oxidizing bacteria (*Methylocaldum*) (Bodrossy et al., 1997) also appeared when *Dolichospermum* and *Synechococcus* were dominant cyanobacterial species (Fig. 6**A**). These methanogens and methanotrophs may contribute to the carbon cycle via methane in the water column of GLSM, even under oxygen-rich environments (Grossart et al., 2011). In addition, *Methanobacterium, Methanosarcina*, and *Methylocaldum* are known for their nitrogen fixation capability (Dos Santos et al., 2012; Leigh, 2000), suggesting their potential association with cyanobacteria like *Synechococcus* as shown in the network (Fig. 6**B**). The network analysis also revealed a potential association between anaerobic ammonium-oxidizing (anammox) bacteria (Planctomycete) and methanotrophic bacteria (*Methylosinus*) in the context of HABs (Fig. 6**B**), although anammox bacteria are observed ubiquitously in lake systems (Xue et al., 2017). This uncovers the potential role of methanogens and anammox bacteria through carbon-nitrogen exchange and cycling, offering additional insights in deciphering microbial dynamics (Fig. 7).

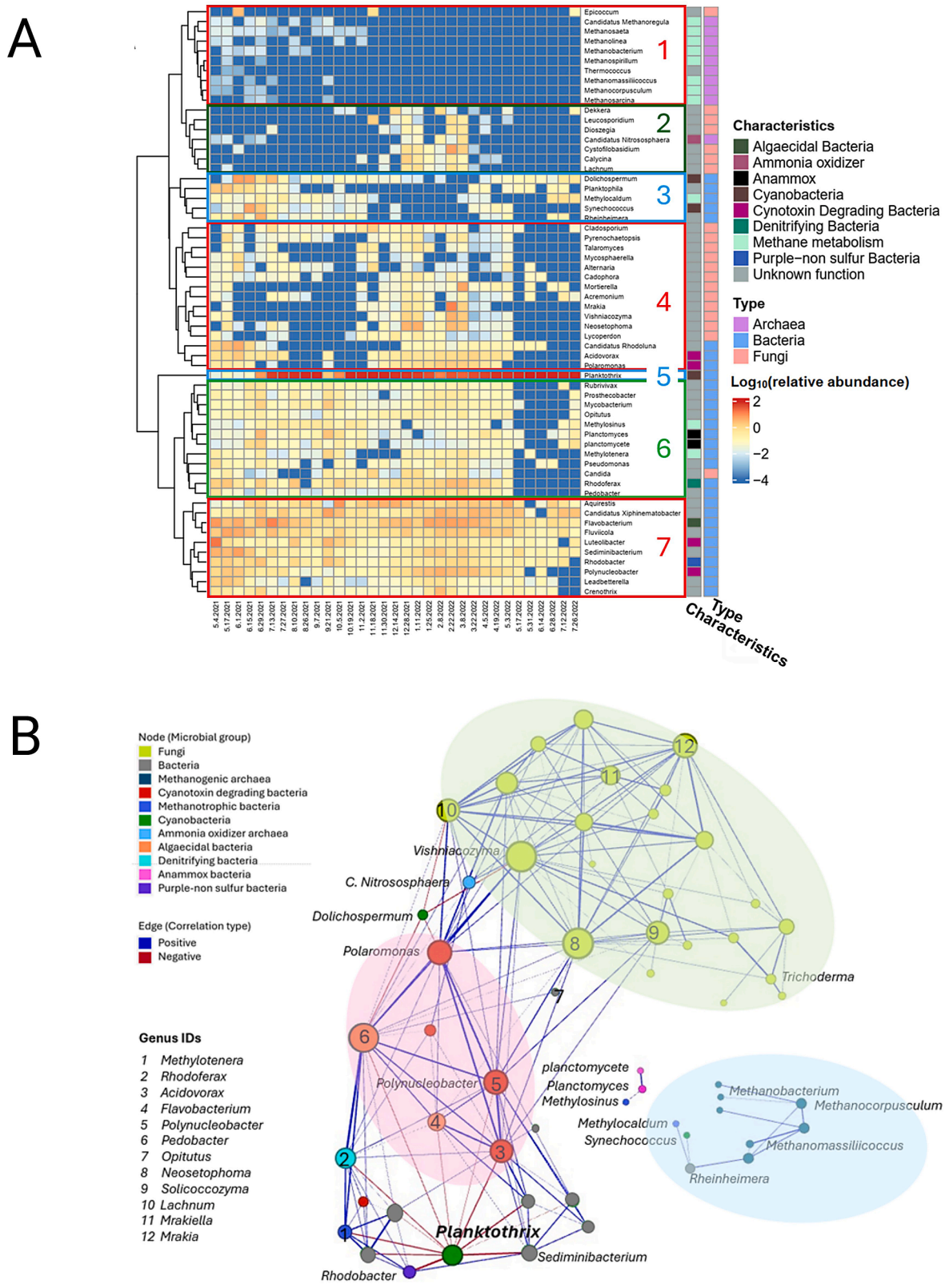

Fig. 6. Heatmap and network analysis of complex microbial interactions. (A) Time series heatmap analysis of archaeal, fungal and bacterial relative abundance in GLSM where the color annotation shows type (as Domain or Kingdom), characteristics (grouped as with known metabolic or functional properties) and (B) Network map of interactions between different bacterial, fungal and archaeal groups considering correlation strength as $|r| > 0.6$ among them.

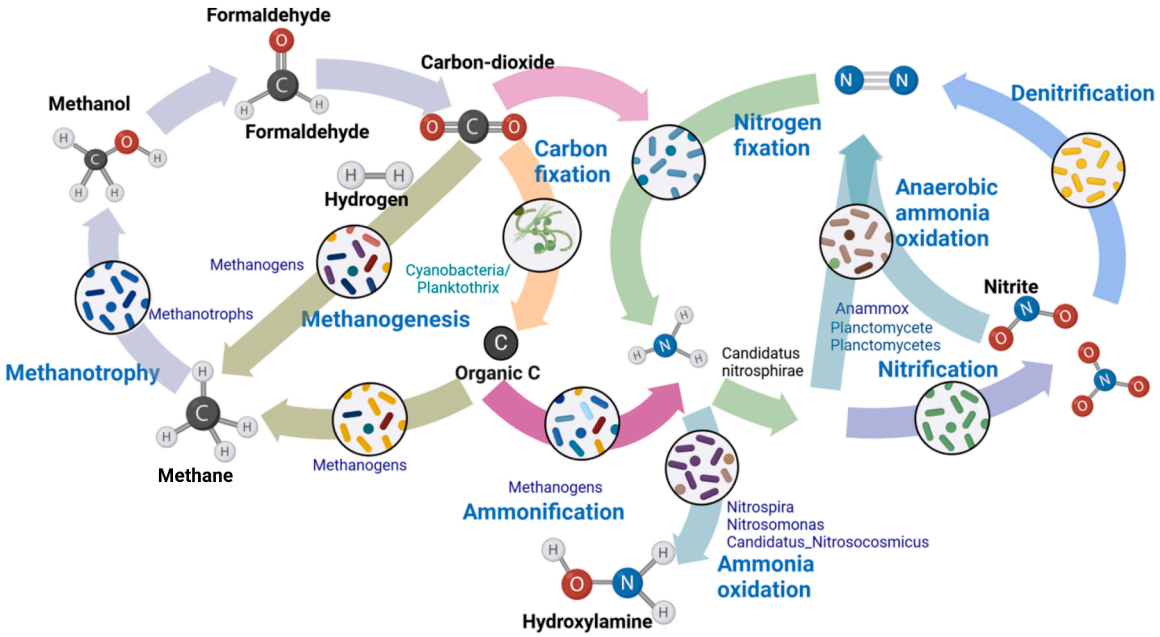

Fig. 7. A schematic diagram of interaction between bacteria and archaea, which shows their possible interaction through carbon and nitrogen metabolism. The events of methanotrophy, methanogenesis, carbon fixation in carbon cycle in the left and nitrogen fixation, ammonia oxidation, nitrification and anaerobic ammonia oxidation, and denitrification are being shown in the right. Here carbon-dioxide from carbon cycles can be used by nitrogen fixing cyanobacteria that can produce ammonia, and organic carbon can be utilized by the methanogens who can take part in the ammonification process to produce ammonia, both of which serve as the links between carbon and nitrogen cycles. Gray color indicates methanotrophy, olive green indicates methanogenesis, orangish indicates carbon fixation, greenish indicates nitrogen fixation, violet color indicates nitrification, turquoise indicates ammonia oxidation, blue indicates denitrification, and pink color indicates links between carbon and nitrogen cycles.

3.6. Ecological insights into microbial interaction during Planktothrix bloom

Our study examined the *Planktothrix* bloom, focusing on the microbial community dynamics and metabolism to identify potential early warning biomarkers. First, this research suggests that the initial bloom was triggered by nitrogen fixation from diazotrophic cyanobacteria. The subsequent input of external nitrogen and phosphorus may have shifted dominance to non-nitrogen-fixing *Planktothrix*, and *Planktothrix* maintained its dominance and toxin production until nitrogen availability declined. Davis et al. (2015) reported that nitrogen supply plays an important role in toxicity in phosphorus-rich system, which aligns well with our observation of toxin concentrations during both the initial bloom and the end phase of the surveillance period. The shift in the cyanobacterial bloom was investigated in the context of nitrogen-fixation by diazotrophic cyanobacteria; however more intricate interactions among bacteria, archaea, and eukaryotes also seem to be involved. The presence of diazotrophic methane metabolizers adds complexity to the dynamics of nitrogen fixation, and carbon dioxide produced by methanotrophs could contribute the growth of both cyanobacteria and ammonia oxidizing archaea as their primary carbon source. Symbiotic relationships that couple carbon and nitrogen cycles have been also recognized in various ecosystems such as a wetland for greenhouse emission (Chen et al., 2020) and an oligotrophic water body for the cnidarian-algal symbiosis (Rädecker et al., 2023). Although not included in Fig. 7, we also unveiled the potential role of fungi against cyanobacteria, aligning with algaecidal and microcystin-degrading bacteria. Activity of algaecidal bacteria, such as *Pedobacter*, can cause the release of toxins, providing an opportunity for toxin degraders (e.g., *Poloromonas, Polynuclobacter*, and *Acidovorax*) and fungi to utilize cyanobacteria-derived nutrients (Fig. 6**B**).

Planktothrix is known to adapt to and thrive in different conditions, but there remain significant knowledge gaps regarding how bloom-forming cyanobacteria contribute to ecosystems. Scheffer et al. (1997) reported sudden and intense outbreak of *P. agardhii* and *P. rubescens* in Lake Vrutci and suggested their potential roles as niche constructors that modify the physiochemical conditions of the water column (Kurmayer et al., 2016). *Planktothrix* manipulates its niche and control community dynamics with secondary metabolites and metabolic property, which allows it to persist bloom for multiple months (Hamre et al., 2018). Thus, *Planktothrix* may act as ecosystem engineers through bioactive secondary metabolite production and thereby posing either adverse or beneficial effects to the neighboring microbial groups such as heterotrophic-toxin degrading bacteria (Kurmayer et al., 2016).

Our findings through DNA-based sequencing data highlights possible interactions among cyanobacteria, fungi, and archaea in *Planktothrix* blooms progression, persistence, and toxicity. However, metatranscriptomic analysis, based on actual gene expression, should be performed to confirm the functional diversity that we observed. We also underscore the need for 18S rRNA gene sequencing analysis to extend the dynamics of the eukaryotes beyond fungal community, which also play significant roles in nutrient cycling and through competition and/or synergism. The availability of viral DNA sequencing data could shed light on the role of cyanophages in cyanobacterial predation. As of an early warning for *Planktothrix* bloom, *Rhodobacter* emerged as a promising candidate biomarker for the *Planktothrix*-dominated bloom. Through multiple seasons over two years, the microbial dynamics and interactions might be affected by the changes of complex physicochemical parameters as well as nutrient level fluctuations. In fact, our beta diversity analysis through unweighted UniFrac metrics showed clear separation of microbiome even in consecutive 2021 and 2022 (**Fig. S6A**) and minimal distinct separation across seasons (**Fig. S6B**). Nonetheless, the opposing pattern between *Planktothrix* and *Rhodobacter* was consistently significant in both years. This identification would provide new tools for the early detection and management of harmful algal blooms, potentially improving water quality protection. Its significant negative association with *Planktothrix* is intriguing, and further laboratory-scale experiments are warranted to confirm the antagonistic

relation between *Rhodobacter* and *Planktothrix* and verify *Rhodobacter*'s functional role within the bloom. Finally, while we employed continuous biweekly sampling during the monitoring period, this approach may have missed to capture sudden changes in the microbial dynamics or diel variations. Moreover, the relatively small number of samples per season (n = 2–7) limited our ability to resolve seasonal patterns and conduct detailed statistical analyses of bloom dynamics. Future studies with more frequent sampling effort needs to validate our observation in shallow, hypereutrophic inland lake, like GLSM.

4. Conclusion

This comprehensive study of Grand Lake St. Marys offers valuable insights into the dynamics of microbial communities within *Planktothrix*-dominated cyanobacterial blooms, which adversely affect water quality and local economies. Our research emphasizes the crucial role of nitrogen metabolism in regulating the dominance of *Planktothrix,* demonstrating that shifts in nitrogen availability significantly influence bloom dynamics through interactions with nitrogen-fixing bacteria, ammonia-oxidizing archaea, anammox, and denitrifying bacteria. During the monitoring period, we observed that *Planktothrix* interacts with a variety of microbes, including bacteria and fungi with algaecidal properties, as well as archaea involved in nutrient cycling. Notably, interactions between toxin-degrading bacteria and algaecidal fungi may indicate a natural regulatory mechanism against harmful algal blooms. Additionally, metagenomic analyses revealed that bloom-associated microbial communities exhibit dynamic shifts in metabolic pathways, including enhanced carbohydrate, nitrogen, sulfur, amino acid, and lipid metabolism, strongly linked to increased toxin production during bloom peaks. We also identified potential interactions between the carbon and nitrogen cycles, involving methane-related bacteria and archaea with nitrogen fixation potential. This study uniquely identified *Rhodobacter* as a signature microbe that may potentially serve as a biomarker for *Planktothrix*-blooms, which would be beneficial for reservoir management and water treatment facilities. Overall, this research advances our knowledge of microbial ecology in cyanobacterial blooms and lays the groundwork for future studies aimed at sustainably managing freshwater resources. By tracing bloom progression and characteristics using early warning biomarkers, water treatment authorities can make informed decisions to ensure effective toxin removal and the provision of safe drinking water.

CRediT authorship contribution statement

Mashuk Siddiquee: Writing – review & editing, Writing – original draft, Visualization, Methodology, Data curation, Conceptualization. **Sara Cornelius:** Investigation. **Youngwoo Seo:** Writing – review & editing, Funding acquisition. **George S. Bullerjahn:** Writing – review & editing. **Thomas B. Bridgeman:** Writing – review & editing, Supervision, Resources, Investigation, Funding acquisition. **Mike Sudman Jr.:** Resources. **Dae-Wook Kang:** Writing – review & editing, Visualization, Validation, Supervision, Investigation, Funding acquisition, Conceptualization.

Declaration of competing interest

The authors declare that they have no known competing financial interests or personal relationships that could have appeared to influence the work reported in this paper.

Acknowledgement

This research was funded by the U.S. Army Engineer Research Development Center, Aquatic Nuisance Species Research Program's HAB Research & Development Initiative, grant W912HZ2120015. We acknowledge the continuous support of the Celina Water Treatment Plant personnel for collecting and shipping the water samples; the contribution of post-doctoral researcher Dr. Youchul Jeon for the development of analytical methods; Gavin Schaeffer, Kristen Hall, Lou Trois, and Vansh Patel for their assistance in sample processing; and Shadman Sakib Sayem for sharing data from the co-culture experiment. We also thank the Bullerjahn lab at Bowling Green State University for sharing their DMSO based chlorophyll-a extraction protocol.

Supplementary materials

Supplementary material associated with this article can be found, in the online version, at doi:10.1016/j.watres.2025.123683.

Data availability

The datasets used during the study are available from the corresponding author upon reasonable request.

References

Al-Tebrineh, J., Mihali, T.K., Pomati, F., Neilan, B.A., 2010. Detection of saxitoxin-producing cyanobacteria and anabaena circinalis in environmental water blooms by quantitative PCR. Appl. Environ. Microbiol. 76 (23), 7836–7842.

Al-Tebrineh, J., Pearson, L.A., Yasar, S.A., Neilan, B.A., 2012. A multiplex qPCR targeting hepato-and neurotoxigenic cyanobacteria of global significance. Harmful. Algae 15, 19–25.

Babele, P.K., Srivastava, A., Young, J.D., 2023. Metabolic flux phenotyping of secondary metabolism in cyanobacteria. Trends Microbiol. 31 (11), 1118–1130.

Bagatini, I.L., Eiler, A., Bertilsson, S., Klaveness, D., Tessarolli, L.P., Vieira, A.A.H., 2014. Host-specificity and dynamics in bacterial communities associated with bloom-forming freshwater phytoplankton. PLoS. One 9 (1), e85950.

Barnard, M.A., Chaffin, J.D., Plaas, H.E., Boyer, G.L., Wei, B., Wilhelm, S.W., Rossignol, K.L., Braddy, J.S., Bullerjahn, G.S., Bridgeman, T.B., 2021. Roles of nutrient limitation on western Lake Erie cyanoHAB toxin production. Toxins (Basel) 13 (1), 47.

Beghini, F., McIver, L.J., Blanco-Míguez, A., Dubois, L., Asnicar, F., Maharjan, S., Mailyan, A., Manghi, P., Scholz, M., Thomas, A.M., 2021. Integrating taxonomic, functional, and strain-level profiling of diverse microbial communities with bioBakery 3. Elife 10, e65088.

Berg, K.A., Lyra, C., Sivonen, K., Paulin, L., Suomalainen, S., Tuomi, P., Rapala, J., 2009. High diversity of cultivable heterotrophic bacteria in association with cyanobacterial water blooms. ISME J. 3 (3), 314–325.

Berry, M.A., Davis, T.W., Cory, R.M., Duhaime, M.B., Johengen, T.H., Kling, G.W., Marino, J.A., Den Uyl, P.A., Gossiaux, D., Dick, G.J., 2017. Cyanobacterial harmful algal blooms are a biological disturbance to Western Lake Erie bacterial communities. Environ. Microbiol. 19 (3), 1149–1162.

Beversdorf, L.J., Miller, T.R., McMahon, K.D., 2013. The role of nitrogen fixation in cyanobacterial bloom toxicity in a temperate, eutrophic lake. PLoS. One 8 (2), e56103.

Bodrossy, L., Holmes, E.M., Holmes, A.J., Kovács, K.L., Murrell, J.C., 1997. Analysis of 16S rRNA and methane monooxygenase gene sequences reveals a novel group of thermotolerant and thermophilic methanotrophs, *Methylocaldum gen. nov*. Arch. Microbiol. 168, 493–503.

Bolyen, E., Rideout, J.R., Dillon, M.R., Bokulich, N.A., Abnet, C.C., Al-Ghalith, G.A., Alexander, H., Alm, E.J., Arumugam, M., Asnicar, F., 2019. Reproducible, interactive, scalable and extensible microbiome data science using QIIME 2. Nat. Biotechnol. 37 (8), 852–857.

Briand, E., Gugger, M., François, J.-C., Bernard, C., Humbert, J.-F., Quiblier, C., 2008. Temporal variations in the dynamics of potentially microcystin-producing strains in a bloom-forming *Planktothrix agardhii* (cyanobacterium) population. Appl. Environ. Microbiol. 74 (12), 3839–3848.

Caporaso, J.G., Lauber, C.L., Walters, W.A., Berg-Lyons, D., Lozupone, C.A., Turnbaugh, P.J., Fierer, N., Knight, R., 2011. Global patterns of 16S rRNA diversity at a depth of millions of sequences per sample. Proc. Natl. Acad. Sci. 108 (Supplement 1), 4516–4522.

Carmichael, W.W., 2001. Health effects of toxin-producing cyanobacteria:"the CyanoHABs. Hum. Ecol. Risk Assess.: Int. J. 7 (5), 1393–1407.

Caspi, R., Altman, T., Billington, R., Dreher, K., Foerster, H., Fulcher, C.A., Holland, T.A., Keseler, I.M., Kothari, A., Kubo, A., 2014. The MetaCyc database of metabolic pathways and enzymes and the BioCyc collection of Pathway/Genome databases. Nucleic Acids Res. 42 (D1), D459–D471.

Chaffin, J.D., Bridgeman, T.B., 2014. Organic and inorganic nitrogen utilization by nitrogen-stressed cyanobacteria during bloom conditions. J. Appl. Phycol. 26, 299–309.

Chen, M., Chang, L., Zhang, J., Guo, F., Vymazal, J., He, Q., Chen, Y., 2020. Global nitrogen input on wetland ecosystem: the driving mechanism of soil labile carbon and nitrogen on greenhouse gas emissions. Environ. Sci. Ecotechnol. 4, 100063.

Cheung, M.Y., Liang, S., Lee, J., 2013. Toxin-producing cyanobacteria in freshwater: a review of the problems, impact on drinking water safety, and efforts for protecting public health. J. Microbiol. 51, 1–10.
da Silva, A.V., da Silva, M.K., de Oliveira, A.J., Silva, J.V., Paulino, S.S., de Queiroz, A.C., Leite, J., França, P.H.B., Putzke, J., Montone, R., 2022. Phosphate solubilization by Antarctic yeasts isolated from lichens. Arch. Microbiol. 204 (12), 698.
Davis, T.W., Bullerjahn, G.S., Tuttle, T., McKay, R.M., Watson, S.B., 2015. Effects of increasing nitrogen and phosphorus concentrations on phytoplankton community growth and toxicity during *Planktothrix* blooms in Sandusky Bay, Lake Erie. Environ. Sci. Technol. 49 (12), 7197–7207.
DeSantis, T.Z., Hugenholtz, P., Larsen, N., Rojas, M., Brodie, E.L., Keller, K., Huber, T., Dalevi, D., Hu, P., Andersen, G.L., 2006. Greengenes, a chimera-checked 16S rRNA gene database and workbench compatible with ARB. Appl. Environ. Microbiol. 72 (7), 5069–5072.
Dewine, M., Stevenson, L.A., 2020. Public Water System Harmful Algal Bloom Response Strategy. Ohio Environmental Protection Agency.
do Amaral, S.C., Xavier, L.P., Vasconcelos, V., Santos, A.V., 2023. Cyanobacteria: a promising source of antifungal metabolites. Mar. Drugs 21 (6), 359.
Dos Santos, P.C., Fang, Z., Mason, S.W., Setubal, J.C, Dixon, R., 2012. Distribution of nitrogen fixation and nitrogenase-like sequences amongst microbial genomes. BMC. Genomics. 13, 1–12.
Dumouchelle, D.H., Stelzer, E.A., 2014. Chemical and biological quality of water in Grand Lake St. Marys, Ohio, 2011–12, with emphasis on cyanobacteria. US Geol. Surv. Sci. Investig. Rep 5210.
Ferber, L., Levine, S., Lini, A., Livingston, G., 2004. Do cyanobacteria dominate in eutrophic lakes because they fix atmospheric nitrogen? Freshw. Biol. 49 (6), 690–708.
Filbrun, J.E., Conroy, J.D., Culver, D.A., 2013. Understanding seasonal phosphorus dynamics to guide effective management of shallow, hypereutrophic Grand Lake St. Marys, Ohio. Lake Reserv. Manag. 29 (3), 165–178.
Foysal, M.J., Timms, V., Neilan, B.A., 2024. Dynamics of the benthic and planktic microbiomes in a *Planktothrix*-dominated toxic cyanobacterial bloom in Australia. Water Res. 249, 120980.
Gobler, C.J., Burkholder, J.M., Davis, T.W., Harke, M.J., Johengen, T., Stow, C.A., Van de Waal, D.B., 2016. The dual role of nitrogen supply in controlling the growth and toxicity of cyanobacterial blooms. Harmful. Algae 54, 87–97.
Gorham, T., Jia, Y., Shum, C., Lee, J., 2017. Ten-year survey of cyanobacterial blooms in Ohio's waterbodies using satellite remote sensing. Harmful. Algae 66, 13–19.
Grossart, H.-P., Frindte, K., Dziallas, C., Eckert, W., Tang, K.W., 2011. Microbial methane production in oxygenated water column of an oligotrophic lake. Proc. Natl. Acad. Sci. 108 (49), 19657–19661.
Guo, D., Liang, J., Chen, W., Wang, J., Ji, B., Luo, S., 2021. Bacterial community analysis of two neighboring freshwater lakes originating from one lake. Pol. J. Environ. Stud 30, 111–117.
Hampel, J.J., McCarthy, M.J., Neudeck, M., Bullerjahn, G.S., McKay, R.M.L., Newell, S. E., 2019. Ammonium recycling supports toxic *planktothrix* blooms in Sandusky Bay, Lake Erie: evidence from stable isotope and metatranscriptome data. Harmful. Algae 81, 42–52.
Hamre, K.D., Lofton, M.E., McClure, R.P., Munger, Z.W., Doubek, J.P., Gerling, A.B., Schreiber, M.E., Carey, C.C., 2018. In situ fluorometry reveals a persistent, perennial hypolimnetic cyanobacterial bloom in a seasonally anoxic reservoir. Freshwater Sci. 37 (3), 483–495.
Hiraishi, A., Yanase, A., Kitamura, H., 1991. Polyphosphate accumulation by *Rhodobacter sphaeroides* grown under different environmental conditions with special emphasis on the effect of external phosphate concentrations. Bull. Japan. Soc. Microbial Ecol. 6 (1), 25–32.
Howarth, R.W., Marino, R., Cole, J.J., 1988. Nitrogen fixation in freshwater, estuarine, and marine ecosystems. 2. Biogeochemical controls. Limnol. Oceanogr. 33 (4), 688–701.
Hoefel, D., Adriansen, C.M., Bouyssou, M.A., Saint, C.P., Newcombe, G., Ho, L., 2009. Development of an mlrA gene-directed TaqMan PCR assay for quantitative assessment of microcystin-degrading bacteria within water treatment plant sand filter biofilms. Appl. Environ. Microbiol. 75 (15), 5167–5169.
Huisman, J., Codd, G.A., Paerl, H.W., Ibelings, B.W., Verspagen, J.M., Visser, P.M., 2018. Cyanobacterial blooms. Nature Rev. Microbiol. 16 (8), 471–483.
Jacquemin, S.J., Doll, J.C., Johnson, L.T., Newell, S.E., 2023. Exploring long-term trends in microcystin toxin values associated with persistent harmful algal blooms in Grand Lake St Marys. Harmful. Algae 122, 102374.
Kahn, A., Oliveira, P., Cuau, M., Leão, P.N., 2023. Incorporation, fate, and turnover of free fatty acids in cyanobacteria. FEMS Microbiol. Rev. 47 (2), fuad015.
Kanehisa, M., Goto, S., 2000. KEGG: kyoto encyclopedia of genes and genomes. Nucleic Acids Res. 28 (1), 27–30.
Kasalický, V., Jezbera, J., Hahn, M.W., Šimek, K., 2013. The diversity of the *Limnohabitans* genus, an important group of freshwater bacterioplankton, by characterization of 35 isolated strains. PLoS. One 8 (3), e58209.
Kharwar, S., Mishra, A.K., 2023. Nitrogen and redox metabolism in cyanobacterium *anabaena sp. PCC 7120* exposed to different sulfate regimes. Curr. Microbiol. 80 (8), 265.
Kim, M., Lee, J., Yang, D., Park, H.Y., Park, W., 2020. Seasonal dynamics of the bacterial communities associated with cyanobacterial blooms in the Han River. Environ. Pollut. 266, 115198.
Klipp, W., Masepohl, B., Pühler, A., 1988. Identification and mapping of nitrogen fixation genes of *Rhodobacter capsulatus*: duplication of a *nifA-nifB* region. J. Bacteriol. 170 (2), 693–699.
Krysenko, S., Wohlleben, W., 2022. Polyamine and ethanolamine metabolism in bacteria as an important component of nitrogen assimilation for survival and pathogenicity. Med. Sci. 10 (3), 40.
Kurmayer, R., Blom, J.F., Deng, L., Pernthaler, J., 2015. Integrating phylogeny, geographic niche partitioning and secondary metabolite synthesis in bloom-forming *Planktothrix*. ISME J. 9 (4), 909–921.
Kurmayer, R., Deng, L., Entfellner, E., 2016. Role of toxic and bioactive secondary metabolites in colonization and bloom formation by filamentous cyanobacteria *Planktothrix*. Harmful. Algae 54, 69–86.
Laezza, C., Salbitani, G., Carfagna, S., 2022. Fungal contamination in microalgal cultivation: biological and biotechnological aspects of fungi-microalgae interaction. J. Fungi 8 (10), 1099.
Leigh, J.A., 2000. Nitrogen fixation in methanogens: the archaeal perspective. Curr. Issues Mol. Biol. 2 (4), 125–131.
Li, H., Bhattarai, B., Barber, M., Goel, R., 2023. Stringent response of cyanobacteria and other bacterioplankton during different stages of a harmful cyanobacterial bloom. Environ. Sci. Technol. 57 (42), 16016–16032.
Ma, J., Qin, B., Wu, P., Zhou, J., Niu, C., Deng, J., Niu, H., 2015. Controlling cyanobacterial blooms by managing nutrient ratio and limitation in a large hyper-eutrophic lake: Lake Taihu, China. J. Environ. Sci. 27, 80–86.
Massey, I.Y., Yang, F., 2020. A mini review on microcystins and bacterial degradation. Toxins (Basel) 12 (4), 268.
McKindles, K.M., Jorge, A.N., McKay, R.M., Davis, T.W., Bullerjahn, G.S., 2021a. Isolation and characterization of rhizophydiales (Chytridiomycota), obligate parasites of *planktothrix agardhii* in a Laurentian Great Lakes embayment. Appl. Environ. Microbiol. 87 (4), e02308–e02320.
McKindles, K.M., Manes, M.A., McKay, R.M., Davis, T.W., Bullerjahn, G.S., 2021b. Environmental factors affecting chytrid (Chytridiomycota) infection rates on *Planktothrix agardhii*. J. Plankton Res. 43 (5), 658–672.
McKindles, K.M., McKay, R.M., Bullerjahn, G.S., 2022. Genomic comparison of *Planktothrix agardhii* isolates from a Lake Erie embayment. PLoS. One 17 (8), e0273454.
Mishra, R.K., 2023. Fresh water availability and its global challenge. Brit. J. Multidiscip. Adv. Stud. 4 (3), 1–78.
Moisander, P., Steppe, T., Hall, N., Kuparinen, J., Paerl, H., 2003. Variability in nitrogen and phosphorus limitation for Baltic Sea phytoplankton during nitrogen-fixing cyanobacterial blooms. Mar. Ecol. Prog. Ser. 262, 81–95.
Nilsson, R.H., Larsson, K.-H., Taylor, A.F.S., Bengtsson-Palme, J., Jeppesen, T.S., Schigel, D., Kennedy, P., Picard, K., Glöckner, F.O., Tedersoo, L., 2019. The UNITE database for molecular identification of fungi: handling dark taxa and parallel taxonomic classifications. Nucleic Acids Res. 47 (D1), D259–D264.
Ohio, E. 2015 Ohio EPA Total (Extracellular and Intracellular) microcystins-ADDA by ELISA Analytical methodology.
Otten, T.G., Paerl, H.W., 2015. Health effects of toxic cyanobacteria in US drinking and recreational waters: our current understanding and proposed direction. Curr. Environ. Health Rep. 2, 75–84.
Özbayram, E.G., Köker, L., Akcaalan, R., Orhan, İ., Albay, M., 2020. Bacterial community composition of Sapanca Lake during a cyanobacterial bloom. Aquatic Sci. Eng. 35 (2), 52–56.
Padisák, J., Crossetti, L.O., Naselli-Flores, L., 2009. Use and misuse in the application of the phytoplankton functional classification: a critical review with updates. Hydrobiologia 621, 1–19.
Paerl, H.W., Fulton, R.S., Moisander, P.H., Dyble, J., 2001. Harmful freshwater algal blooms, with an emphasis on cyanobacteria. Sci. World J. 1, 76–113.
Paerl, H.W., Hall, N.S., Calandrino, E.S., 2011. Controlling harmful cyanobacterial blooms in a world experiencing anthropogenic and climatic-induced change. Sci. Total Environ. 409 (10), 1739–1745.
Perini, L., Gostinčar, C., Anesio, A.M., Williamson, C., Tranter, M., Gunde-Cimerman, N., 2019. Darkening of the Greenland Ice Sheet: fungal abundance and diversity are associated with algal bloom. Front. Microbiol. 10, 557.
Pineda-Mendoza, R.M., Briones-Roblero, C.I., Gonzalez-Escobedo, R., Rivera-Orduña, F. N., Martínez-Jerónimo, F., Zúñiga, G., 2020. Seasonal changes in the bacterial community structure of three eutrophicated urban lakes in Mexico city, with emphasis on *microcystis spp*. Toxicon. 179, 8–20.
Rädecker, N., Escrig, S., Spangenberg, J.E., Voolstra, C.R., Meibom, A., 2023. Coupled carbon and nitrogen cycling regulates the cnidarian–algal symbiosis. Nat. Commun. 14 (1), 6948.
Reinl, K.L., Harris, T.D., North, R.L., Almela, P., Berger, S.A., Bizic, M., Burnet, S.H., Grossart, H.P., Ibelings, B.W., Jakobsson, E., 2023. Blooms also like it cold. Limnol. Oceanogr. Lett. 8 (4), 546–564.
Ren, X., Whitton, M.M., Trotter, T., Ashwath, N., Stanley, D., Bajagai, Y.S., 2024. Enhancing soil health and carbon sequestration through phytogenic treatment: insights into microbial functional pathways in pasture dieback affected soil. Plant Soil 1–17.
Reynolds, C.S., Huszar, V., Kruk, C., Naselli-Flores, L., Melo, S., 2002. Towards a functional classification of the freshwater phytoplankton. J. Plankton Res. 24 (5), 417–428.
Rücker, J., Wiedner, C., Zippel, P., 1997. Shallow Lakes' 95. Springer, pp. 107–115.
Rusinova-Videva, S., Ognyanov, M., Georgiev, Y., Kambourova, M., Adamov, A., Krasteva, V., 2022. Production and chemical characterization of exopolysaccharides by antarctic yeasts *Vishniacozyma victoriae* and *Tremellomycetes sp*. Appl. Sci. 12 (4), 1805.
Salcher, M.M., Neuenschwander, S.M., Posch, T., Pernthaler, J., 2015. The ecology of pelagic freshwater methylotrophs assessed by a high-resolution monitoring and isolation campaign. ISME J. 9 (11), 2442–2453.

Scheffer, M., Rinaldi, S., Gragnani, A., Mur, L.R., van Nes, E.H., 1997. On the dominance of filamentous cyanobacteria in shallow, turbid lakes. Ecology. 78 (1), 272–282.
Schmidt, J.R., Shaskus, M., Estenik, J.F., Oesch, C., Khidekel, R., Boyer, G.L., 2013. Variations in the microcystin content of different fish species collected from a eutrophic lake. Toxins (Basel) 5 (5), 992–1009.
Sethuraman, A., Stancheva, R., Sanders, C., Caceres, L., Castro, D., Hausknecht-Buss, H., Henry, S., Johansen, H., Kasler, A. and Lastor, S. 2022. Genome of a novel *sediminibacterium* discovered in association with two species of freshwater cyanobacteria from streams in Southern California. G3 12(7), jkac123.
Smith, D.P., Peay, K.G., 2014. Sequence depth, not PCR replication, improves ecological inference from next generation DNA sequencing. PLoS. One 9 (2), e90234.
Smith, V.H., 1983. Low nitrogen to phosphorus ratios favor dominance by blue-green algae in lake phytoplankton. Science (1979) 221 (4611), 669–671.
Steffen, M.M., Li, Z., Effler, T.C., Hauser, L.J., Boyer, G.L., Wilhelm, S.W., 2012. Comparative metagenomics of toxic freshwater cyanobacteria bloom communities on two continents. PLoS. One 7 (8).
Steffen, M.M., Zhu, Z., McKay, R.M.L., Wilhelm, S.W., Bullerjahn, G.S., 2014. Taxonomic assessment of a toxic cyanobacteria shift in hypereutrophic Grand Lake St. Marys (Ohio, USA). Harmful. Algae 33, 12–18.
Takahashi, H., Kopriva, S., Giordano, M., Saito, K., Hell, R., 2011. Sulfur assimilation in photosynthetic organisms: molecular functions and regulations of transporters and assimilatory enzymes. Annu. Rev. Plant Biol. 62 (1), 157–184.
Toporowska, M., Mazur-Marzec, H., Pawlik-Skowrońska, B., 2020. The effects of cyanobacterial bloom extracts on the biomass, chl-a, MC and other oligopeptides contents in a natural *Planktothrix agardhii* population. Int. J. Environ. Res. Public Health 17 (8), 2881.
Tromas, N., Fortin, N., Bedrani, L., Terrat, Y., Cardoso, P., Bird, D., Greer, C.W., Shapiro, B.J., 2017. Characterising and predicting cyanobacterial blooms in an 8-year amplicon sequencing time course. ISME J. 11 (8), 1746–1763.
Velichko, N., Chernyaeva, E., Averina, S., Gavrilova, O., Lapidus, A., Pinevich, A., 2015. Consortium of the 'bichlorophyllous' cyanobacterium *prochlorothrix hollandica* and chemoheterotrophic partner bacteria: culture and metagenome-based description. Environ. Microbiol. Rep. 7 (4), 623–633.
Viaggiu, E., Melchiorre, S., Volpi, F., Di Corcia, A., Mancini, R., Garibaldi, L., Crichigno, G., Bruno, M., 2004. Anatoxin-a toxin in the cyanobacterium *planktothrix rubescens* from a fishing pond in northern Italy. Environ. Toxicol.: Int. J. 19 (3), 191–197.
Wagner, N.D., Quach, E., Buscho, S., Ricciardelli, A., Kannan, A., Naung, S.W., Phillip, G., Sheppard, B., Ferguson, L., Allen, A., 2021. Nitrogen form, concentration, and micronutrient availability affect microcystin production in cyanobacterial blooms. Harmful. Algae 103, 102002.
Wagner, R.S., McKindles, K.M., Bullerjahn, G.S., 2023. Effects of water movement and temperature on rhizophydium infection of *Planktothrix* in a shallow hypereutrophic lake. Front. Microbiol. 14, 1197394.
Wang, K., Mou, X., Cao, H., Struewing, I., Allen, J., Lu, J., 2021. Co-occurring microorganisms regulate the succession of cyanobacterial harmful algal blooms. Environ. Pollut. 288, 117682.
Wang, Z., Zeng, Y., Cheng, K., Cai, Z., Zhou, J., 2022. The quorum sensing system of *novosphingobium sp. ERN07* regulates aggregate formation that promotes cyanobacterial growth. Sci. Total Environ. 851, 158354.
White, T.J., Bruns, T., Lee, S., Taylor, J., 1990. Amplification and direct sequencing of fungal ribosomal RNA genes for phylogenetics. PCR Protocol.: Guide Method. Appl. 18 (1), 315–322.
Xue, Y., Yu, Z., Chen, H., Yang, J.R., Liu, M., Liu, L., Huang, B., Yang, J., 2017. Cyanobacterial bloom significantly boosts hypolimnelic anammox bacterial abundance in a subtropical stratified reservoir. FEMS Microbiol. Ecol. 93 (10), fix118.
Zepernick, B.N., McKay, R.M.L., Martin, R.M., Bullerjahn, G.S., Paerl, H.W., Wilhelm, S. W., 2024. A tale of two blooms: do ecological paradigms for algal bloom success and succession require revisiting? J. Great Lakes Res., 102336
Zhang, X., Ye, X., Chen, L., Zhao, H., Shi, Q., Xiao, Y., Ma, L., Hou, X., Chen, Y., Yang, F., 2020. Functional role of bloom-forming cyanobacterium *planktothrix* in ecologically shaping aquatic environments. Sci. Total Environ. 710, 136314.
Zhang, Z., Fan, X., Peijnenburg, W., Zhang, M., Sun, L., Zhai, Y., Yu, Q., Wu, J., Lu, T., Qian, H., 2021. Alteration of dominant cyanobacteria in different bloom periods caused by abiotic factors and species interactions. J. Environ. Sci. 99, 1–9.
Zhou, J., Richlen, M.L., Sehein, T.R., Kulis, D.M., Anderson, D.M., Cai, Z., 2018. Microbial community structure and associations during a marine dinoflagellate bloom. Front. Microbiol. 9, 1201.